Available online at BIOMA: Jurnal Ilmiah Biologi
Websites:http://journal.upgris.ac.id/index.php/bioma/index
BIOMA: Jurnal Ilmiah Biologi, 14 (2), October 2025, 73-89
DOI: https://doi.org/10.26877/585f2k97

IN SILICO ANALYSIS ON BINDING ACTION OF TERPENE NATURAL COMPOUNDS FROM APOCYNACEAE FAMILY AGAINST SHV-1 BETA-LACTAMASE OF *Klebsiella pneumoniae*

Sajida AM Sabbah[1], Sri Budiarti[1], Rika Indri Astuti[1,2,3*]
[1]Department of Biology, Faculty of Mathematics and Natural Sciences, Dramaga Campus, Bogor Agricultural University, Bogor 16680, Indonesia.
[2]Biotech Center, Dramaga Campus, Bogor Agricultural University, Bogor, 16680, Indonesia
[3]Biopharmaca Research Center, Taman Kencana Campus, Bogor Agricultural University, Bogor, Indonesia
**Corresponding author:rikaindriastuti@apps.ipb.ac.id*

ARTICLE INFO

Article history

Submission	2025-08-03
Revision	2025-09-02
Accepted	2025-10-14

Keywords:
Alkaloids
Antibiotic resistant
Beta-lactamase
In silico
Klebsiella penumoniae

ABSTRACT

This study investigates the potential of Monoterpene Indole Alkaloids (MIAs) derived from six genera within the Apocynaceae family as inhibitors of the beta-lactamase enzyme (bla-SHV-1), which plays a key role in antibiotic resistance in Klebsiella pneumoniae. Using the PyRx program for molecular docking, we assessed the binding affinity and interaction profiles of various MIAs with bla-SHV-1. Our results identified Paucidisine, (-)-19-Oxoisoeburnamine, and Paucidactine A as the most promising candidates, based on their interaction energies and binding modes. These findings highlight the potential of these specific MIAs as candidates for antibiotic resistance treatment, marking a significant step towards developing alternative treatment options for antibiotic-resistant Klebsiella infections.

INTRODUCTION

Klebsiella pneumoniae, a Gram-negative, nonmotile, encapsulated rod-shaped bacterium, has emerged as a significant nosocomial pathogen causing a variety of clinical infectious diseases, including pneumonia, urinary tract infections, bacteremia, cholecystitis, osteomyelitis, meningitis, and thrombophlebitis (Abbas et al., 2024; Zhu et al., 2021). *The severity of these infections cannot be overstated, with Klebsiella pneumoniae* being the third most common cause of bloodstream infections globally, following *Staphylococcus aureus* and *Escherichia coli* (Ikuta et al., 2022). Infection occurs only when it can evade and overcome the primary and secondary immune

responses of the host, and this is a particularly tangible possibility in hospital settings (Jenkins, 2021; Khan et al., 2017). Over the past decade, the emergence of multiple antibiotic-resistant *K. pneumoniae* has rapidly increased worldwide. This increase is attributed to the frequent and extensive use of antibiotics in hospitals, which leads to the development of resistant strains and severely limits treatment options (Assefa, 2022).

A key protein contributing to antibiotic resistance in *Enterobacteriaceae,* including *Salmonella*, is beta-lactamase (Parawidnyaningsih et al., 2023). Beta-lactamases are a diverse class of enzymes produced by bacteria that inactivate beta-lactam antibiotics by breaking open the beta-lactam ring (Tooke et al., 2019). SHV-type beta-lactamases from *K. pneumoniae* hydrolyze penicillin and cephalosporins, rendering these antibiotics ineffective and contributing significantly to bacterial resistance (Liakopoulos et al., 2016). A previous study observed that the resistant property is not only encoded within the plasmid but also within the chromosomes (Ferdosi-Shahandashti et al., 2024).

Monoterpenes, the smallest of terpenes, are compounds containing C10H16 and are primary components of essential oils derived from various plant parts. Many plants' bioactive compounds, including monoterpenes, have demonstrated antifungal (Vasconcelos et al., 2024), antibacterial, and antiviral (Syarifah et al., 2022). Monoterpene indole alkaloids (MIAs), metabolites with a bicyclic structure comprising a benzene ring fused to a five-membered pyrrole ring, have shown diverse physiological and pharmacological effects (Liu et al., 2019). The Apocynaceae family, which includes genera such as *Alstonia*, *Rauvolfia*, *Kopsia*, *Ervatamia*, *Tabernaemontana*, and *Rhazya*, is noted for producing biologically active natural metabolites, some of which have shown potential as antimicrobial agents. This makes them a promising source for the development of new antibiotics and inhibitors against antibiotic-resistant bacteria like K. pneumoniae (Diekema et al., 2019).

In this study, the effects of MIAs on the SHV-1 protein were evaluated using *in silico* analysis. In silico methods, particularly molecular docking, are computational techniques used to investigate pharmacological hypotheses and design drug therapies by determining interactions between ligands and target molecules (Prasad et al., 2018). Molecular docking has proven to be more accurate than high-throughput screening for drug discovery (Agu et al., 2023). In recent years, *in silico* models have become increasingly popular, and the use of such methods can help identify ways to control the

virulence of pathogenic bacteria, including *K. pneumoniae*. By exploring the potential of MIAs as potent inhibitors of the SHV-1 protein, this study aims to inspire hope and contribute to the development of new treatment strategies for combating antibiotic-resistant *K. pneumoniae* infections. The findings could pave the way for future experimental and clinical research, ultimately enhancing patient outcomes and addressing the global challenge of antibiotic resistance.

MATERIALS AND METHODS

Tools

The computational study employed several specialized software tools, each chosen for its specific role in predicting interactions between ligands and the target protein. These tools included PyRx version 1.1 for molecular docking, PyMOL version 3.1 and UCSF ChimeraX for visualization, YASARA version 18.4.24 for ligand preparation, LigPlot+ version 2.2 for interaction analysis, and Discovery Studio Visualizer 2020 for detailed visualization and analysis. Each of these tools was selected for its unique capabilities and its ability to contribute to the overall understanding of the ligand-protein interactions.

Selection of the target protein and ligand

Selection of the target protein and ligand For the selection of the target protein and ligands, we relied on a strong foundation of previous research. We utilized open-access databases, including PubMed, UniProt, PubChem, DrugBank, SciFinder, and ChEMBL. The beta-lactamase enzyme (bla-SHV-1) from *Klebsiella pneumoniae* was chosen as the target protein due to its role in antibiotic resistance. Monoterpene Indole Alkaloids (MIAs) were selected as potential ligands based on previous research, which identified over 400 MIA compounds (Mohammed et al., 2021). We applied Lipinski's "Rule of Five" to ensure the selected compounds had favorable drug-like properties, demonstrating the strong foundation of our selection process.

Preparation of Target Protein and Ligands

The protein preparation was performed according to the previous protocol (Yuan et al., 2017). The target protein's structure was obtained from the Protein Data Bank (PDB). PyMOL was used to visualize and prepare the protein structure. Chain A and its co-crystal

ligands MA4, EPE, and 1OG were identified. The MA4 and EPE ligands were removed, while the 1OG ligand was retained to facilitate identification of the active site and ensure stability. The prepared protein was then saved in PDB format. Ligand Preparation: Ligand structures were obtained in SDF format from the respective databases and converted to PDB format using YASARA (Sepehri et al., 2022). The ligands were then loaded into PyRx, where energy minimization was performed to optimize their structures. The minimized ligands were saved in PDB format for subsequent docking studies.

Active-Site Determination

Active site determination was performed using PyMOL to identify the receptor regions where the ligands would dock. Two docking methods were employed: a) Targeted Docking: A three-dimensional map of the receptor's active site was created to focus on specific docking (Tallei et al., 2020). b) Blind Docking: A three-dimensional map encompassing the entire receptor SHV-1 was generated to allow docking to all possible receptor sites. These methods ensured a comprehensive analysis of potential binding sites for the ligands (Alfaridza et al., 2025).

Molecular Docking

Docking Procedure: Molecular docking was conducted using PyRx, which utilizes the AutoDock Vina algorithm. Both blind and specific docking were performed in triplicate to ensure reproducibility. The receptor and ligand PDB files were loaded into the software, and docking was executed using the forward command. Docking results were evaluated by selecting the optimal pose with the lowest Gibbs free energy of binding (-ΔG), indicating the highest binding affinity between the ligand and receptor. The configurations were saved in CSV format. Visualization of the docking results was performed using PyMOL and LigPlot++ to identify residues involved in hydrogen bonds and hydrophobic interactions. Validation: The docking method was rigorously validated by redocking the native ligand (7-Alkylidenecephalosporin Sulfones) with the target protein. The method's validity was confirmed by obtaining an RMSD (root-mean-square distance) value ≤ 2 Å, indicating accurate and reliable docking. This thorough validation process reinforces the scientific rigor of the study and assures the reader of the reliability of the results.

RESULTS AND DISCUSSION

Selection of Target Protein and Ligands

The target protein selected for this study is SHV-1, a well-characterized beta-lactamase enzyme that plays a critical role in antibiotic resistance, particularly in *K. pneumoniae*. The 3D structure of SHV-1 was obtained from the Protein Data Bank (PDB ID: 4JPM) (Figure 1). SHV-1 was chosen as a target due to its clinical significance and its role in conferring resistance to beta-lactam antibiotics, making it a relevant target for investigating new antimicrobial agents (Sepehri et al., 2022). From an initial collection of over 400 terpene compounds isolated in previous studies, a subset was meticulously refined using database searches and Lipinski's rule of five (Ro5) criteria. The Lipinski's rule of five is a set of guidelines predicting the drug likeness of a compound, which suggests that poor absorption or permeation is more likely when there are more than five hydrogen bond donors (OH and NH groups), more than ten hydrogen bond acceptors (N and O atoms), a molecular weight greater than 500 Dalton, a partition coefficient log P greater than 5, and molar refractivity outside the range of 40-130.

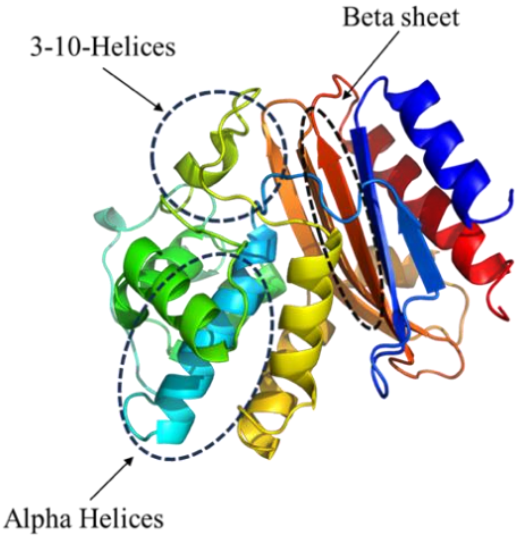

Figure 1. The 3D structure of SHV-1, [PDB ID: 4JPM]. Alpha Helices (the spiral shape), Beta sheet (the arrow shape) and 3-10 Helices (the short structure)

Out of the 180 terpene compounds identified, 130 emerged as potential game-changers. A further screening based on Lipinski's rule, which emphasizes the significance of solubility and permeability, revealed that these 130 compounds did not violate more than one of the Ro5 criteria. This suggests that these compounds are likely

to have favorable pharmacokinetic properties, making them promising candidates for further study. These compounds were prepared as ligands for molecular docking studies, with detailed information presented in Table 1.

Table 1. Ligand parameters to comply with Lipinski's rules

No	Compound Name	CID*	Mass (g/mol)	Log P	H Bond Donor	H Bond Acceptors	Molar Refractivity
1	Scholarisine A	101840191	306.35842	1.6963	0	4	94.169
2	(16R)-E-Isositsnikine	6436828	275.27	2.7527	2	4	105.6635
3	Nareline	24883687	352.3838	1.0856	1	6	100.8088
4	5-Methoxystrictamine	102004590	352.42686	2.1998	0	5	106.568
5	Leuconolam	14442600	326.38958	2.5992	2	5	986.525
6	19-Epischolaricine	14707744	356.41556	1.6633	3	6	103.5665
7	Scholaricine	50900051	356.41556	1.6633	3	6	103.5665
8	Vallesamine	13783712	340.41616	2.2907	2	4	100.7395
9	Akuammidine	15558574	352.42686	2.5051	2	4	103.2895
10	Strictosamide	10345799	498.525	0.4104	5	9	130.6519
11	Methyl Demethoxycarbonylchanofruticosinate	25104767	352.42686	2.1848	1	5	103.5267
12	Singaporentine A	25179277	378.42108	1.9066	0	6	109.541
13	15-Hydroxykopsamine	102314958	428.47822	1.1794	2	8	117.0706
14	Singaporentinidine	102314960	309.38224	2.9737	2	2	943.175
15	Kopsininate	102584119	324.41676	2.9174	2	4	990.065
16	Kopsinilam	21607614	352.42686	2.5324	1	5	103.5267
17	12-Methoxykopsine	102520721	410.46294	1.7089	1	7	114.6548
18	19(R)-Methoxytubotaiwine	23627132	354.44274	2.6118	1	5	106.2737
19	(−)-Eburnamonine	71203	294.39078	3.7125	0	2	922.185
20	Kopsilongine	44326354	442.5048	2.2172	1	8	122.4008
21	Kopsamine	11015920	456.48832	1.9373	1	9	121.9718
22	Arboridinine	122231131	294.39078	2.0466	1	3	955.238
23	Paucidirisine	132966069	390.47484	3.0886	1	5	115.3597
24	Paucidactinine	132966070	440.44586	1.5047	1	9	115.0508
25	Paucidactine B	101699203	454.42938	0.8262	1	10	115.2508
26	paucidactine A	73345269	470.42878	0.1462	2	11	116.4506
27	Paucidisine	132966071	378.42108	2.2561	0	6	106.903
28	(−)-19-Oxoisoeburnamine	139051313	310.39018	2.7422	1	3	931.588
29	(−)-19(R)-Hydroxyeburnamenine	127030478	294.39078	3.1237	1	2	932.768
30	(−)-19(R)-Hydroxy-O-Ethylisoeburnamine	127030479	340.45922	3.5782	1	3	103.6578
31	Paucidactine C	102382648	470.47184	1.1147	1	10	122.1718
32	Eburnamenine	6857502	278.39138	4.1529	0	1	92.115
33	(+)-Isoeburnamine	118701077	296.40666	3.5632	1	2	929.588

No	Compound Name	CID*	Mass (g/mol)	Log P	H Bond Donor	H Bond Acceptors	Molar Refractivity
34	(+)-19-Oxoeburnamine	102445440	310.39018	2.7422	1	3	931.588
35	Arborisidine	132557639	280.3642	2.0871	0	3	90.489
36	Arbornamine	132557640	310.39018	2.0956	2	3	937.896
37	Kopsinidine C	132576284	324.41676	1.5483	3	4	974.823
38	Kopsinidine D	132576285	354.44274	1.5569	3	5	103.9743
39	Kopsinidine E	132576286	368.42626	1.277	3	6	103.5453
40	11,12-Methylenedioxychanofruticosinic Acid	132576287	440.44586	1.913	1	9	116.6518
41	12-Methoxychanofruticosinic Acid	132576288	426.46234	2.1929	1	8	117.0808
42	Chanofruticosinic Acid	132576289	396.43636	2.1843	1	7	110.5888
43	Methyl 11,12-Methylenedioxychanofruticosinate	44326005	396.43636	2.4582	0	7	110.035
44	Kopsininic Acid	102597247	324.41676	2.9174	2	4	990.065
45	(−)-11,12-Methylenedioxykopsinaline	137832348	398.45224	1.8494	2	7	110.5895
46	Kopsinoline	137832351	354.44274	3.0393	1	3	106.6937
47	Kopsinine B	102597920	354.44274	2.1207	2	5	104.5265
48	Rhazinilam	11312435	294.39078	4.467	1	2	930.337
49	Kopsifoline A	12116551	382.45284	2.1104	2	6	110.2465
50	20-Oxoeburnamenine	11279548	350.41098	2.8751	0	4	103.214
51	12-Methylenedioxychanofruticosinate	44326005	396.43636	2.4582	0	7	110.035
52	Oxayohimban-16-Carboxylic Acid	3055759	338.40028	3.0283	2	4	991.525
53	Peraksine	78146432	310.39018	2.3766	2	3	920.955
54	Alstoyunine A	46882285	340.41616	2.3491	2	4	979.875
55	Lochnerine	6436184	324.41676	2.9705	2	3	991.425
56	Serpentinic Acid	73073	348.3951	3.4536	0	4	995.91
57	Ajmalicine	441975	352.42686	3.1167	1	4	103.4727
58	Sitsirikine	5321352	354.44274	2.6086	2	4	105.6635
59	Spegatrine	6441055	325.4247	2.833	3	2	100.5375
60	19(S),20(R)-Dihydroperaksine	636655	312.40606	2.0126	3	3	942.863
61	Coronaridine Hydroxyindolenine	14061706	354.44274	2.0173	1	5	106.8588
62	10-Hydroxycoronaridine	156852	354.44274	2.8987	2	4	104.7677
63	Voacangine	73255	368.46932	3.2017	1	4	109.2367
64	19(S)-Heyneanine	44566752	384.46872	2.1725	2	5	110.3985
65	19(R)-Heyneanine	44566753	384.46872	2.1725	2	5	110.3985
66	Vobasine	320369	352.42686	2.9004	1	4	104.9232

No	Compound Name	CID*	Mass (g/mol)	Log P	H Bond Donor	H Bond Acceptors	Molar Refractivity
67	Ervahainine A	73213144	379.4522	2.52808	1	6	110.1587
68	Iboluteine	21589055	326.43264	3.2584	1	4	101.8322
69	Conopharyngine	453209	398.4953	3.2103	1	5	115.7287
70	Voacristine	196982	384.46872	2.1725	2	5	110.3985
71	3-Oxo-7r-Coronaridine Hydroxyindolenine	139201774	409.47818	2.07378	1	7	118.5358
72	Pseudoindoxyl Coronaridine	102121233	354.44274	2.793	1	5	105.9792
73	Lirofoline A	46184733	324.41676	3.5754	0	3	989.705
74	Lirofoline B	46186635	354.44274	2.9379	1	4	104.9393
75	19-Epi-Voacristine	44566748	400.46812	0.9967	2	7	114.5126
76	Ervatamine	161765	354.44274	2.9819	1	4	105.1372
77	20-Epi-Ervatamine	12308875	354.44274	2.9819	1	4	105.1372
78	Dregamine	99108	354.44274	2.9803	1	4	105.3972
79	Tabernaemontanine	12309360	354.44274	2.9803	1	4	105.3972
80	Isovoacangine	44393473	368.46932	3.2017	1	4	109.2367
81	Conodusine C	132566483	310.39018	3.0784	1	1	955.297
82	Apocidine A	132566484	368.42626	1.8299	2	6	105.0995
83	Apocidine B	132566485	368.42626	1.4807	2	6	105.0615
84	Conoduzidine A	132566486	308.3743	2.7013	0	3	911.895
85	(+)-Catharanthine	5458190	336.42746	3.1132	1	3	102.2707
86	Isoakuammiline	132584660	394.46354	2.1606	0	6	116.122
87	18-Hydroxypseudovincadifformine	132584661	354.44274	2.3494	2	5	106.3505
88	Tubotaiwine	13783720	324.41676	2.9869	1	4	100.3817
89	Voachalotine	11969553	366.45344	2.555	1	4	108.1908
90	Rhazimal	101967159	350.41098	1.7964	0	5	105.423
91	Strictamine-N-Oxide	101407506	338.40028	2.2629	0	3	104.002
92	Akuammicine	10314057	322.40088	2.907	1	4	999.077
93	16R-E-Isositsirikine	6436828	354.44274	2.7527	2	4	105.6635
94	Dihydrositsirikine	5316739	356.45862	2.8326	2	4	106.1375
95	Antirhine	5462421	296.40666	3.2095	2	2	947.645
96	Eburenine	10945856	280.40726	3.4423	0	2	947.98
97	Quebrachamine	92990	282.42314	4.0867	1	1	938.167
98	Strictanol	12314913	298.42254	3.0099	1	3	980.738
99	Strictamine	21159178	322.40088	2.2273	0	4	100.676
100	(−)-Minovincinine	138911111	355.45068	2.7061	3	5	107.0532
101	Echitovenaldine	102090470	426.5054	3.0713	1	7	122.3197
102	Echitovenidine	23650	436.54328	4.009	1	6	129.7747
103	Lochnericine	11382599	352.42686	2.5083	1	5	103.8997
104	Tabersonine	20485	336.42746	3.2971	1	4	104.4547
105	Perakine	453213	350.41098	1.6255	0	5	104.043

No	Compound Name	CID*	Mass (g/mol)	Log P	H Bond Donor	H Bond Acceptors	Molar Refractivity
106	Picrinine	46229104	338.40028	2.3217	1	5	99.3907
107	Picralinal	46229103	366.41038	1.8908	1	6	104.1377
108	Rhazimol	101986486	338.40028	1.5014	2	5	102.0646
109	Alsmaphorazine B	102041783	368.3832	0.4276	1	7	101.5588
110	Oxovincadifformine	101999102	352.42686	3.0477	1	5	105.1287
111	Vinorine	5281974	334.41158	2.3682	0	4	103.369
112	Alsmaphorazine C	101571300	384.42566	1.3304	1	7	107.7458
113	Alsmaphorazine D	101571301	372.41496	0.4454	2	7	103.5116
114	Alsmaphorazine E	101571302	402.44094	0.454	2	8	110.0036
115	Scholarisin I	102226202	396.43636	1.8649	1	7	110.0677
116	Scholarisin II	102226203	398.45224	1.6583	2	7	111.0295
117	Scholarisin III	102226204	440.48892	2.2291	1	8	120.7667
118	Scholarisin IV	102226205	386.44154	1.8442	2	7	106.7854
119	Scholarisin VI	102226207	382.45284	1.4781	1	6	111.2298
120	Scholarisin VII	102226208	382.45284	1.5623	1	6	112.2768
121	(3R,5S,7R,15R,16R,19E)- Scholarisine F	102226209	368.42626	2.2958	1	6	105.3207
122	3-Epi-Dihydrocorymine	102226210	384.46872	1.2715	2	6	112.1916
123	Alstolactine A	101894075	370.39908	0.6955	2	7	101.2645
124	Alstolactine B	101894076	370.39908	0.6955	2	7	101.2645
125	Alstolactine C	101894077	414.45164	0.6209	1	8	112.0578
126	Alistonitrine A	102222299	367.4415	1.386	1	6	109.4067
127	Alstonerinal	71720002	336.42746	3.153	0	3	102.482
128	Alstonerine	10382386	336.42746	3.153	0	3	102.482
129	(−)-Eburnamine	101699	296.40666	3.5632	1	2	929.588
130	Methyl Chanofruticosinate	91895274	410.46294	2.2727	0	7	114.909

* CID = Chemical Identifier from PubChem

Docking Validation

To validate the docking protocol used in this study, a redocking approach was employed. This approach is significant as it involves docking the native ligand back into the SHV-1 receptor, thereby assessing the accuracy of the docking method. The redocking process was performed using the defined binding site coordinates: X = 11.729, Y = 37.5, and Z = -1.2519. The results of this validation are depicted in Figure 2.

One of the key parameters for evaluating the accuracy of docking simulations is the Root Mean Square Deviation (RMSD). An RMSD value within 3.0 Å is generally considered acceptable, indicating that the docking method can reliably reproduce the native ligand binding mode and the accuracy of ligand-protein interactions (Meng et al.,

2011; Ramírez & Caballero, 2018). The RMSD value obtained from the redocking of the native ligand with the SHV-1 receptor was found to be 3.8 Å. Although slightly above the typically acceptable threshold of 3.0 Å, this value suggests that the docking method used in this study is nearly acceptable for predicting ligand-protein interactions. This RMSD indicates that, although the docking protocol may exhibit minor deviations, it remains capable of providing reasonably accurate predictions of the ligand binding poses within the active site of SHV-1. The nearly acceptable RMSD value highlights the potential of this validation step and underscores the need for further optimization of the docking parameters to enhance accuracy. Nonetheless, the docking method employed in this study is sufficient to provide insights into the potential interactions between terpene compounds and the SHV-1 receptor, supporting the subsequent analysis of docking results and interpretation of ligand efficacy.

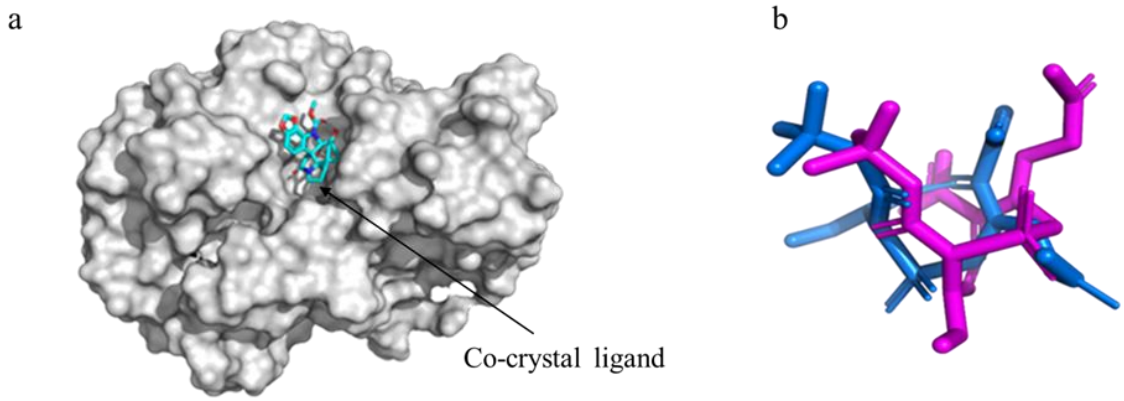

Figure 2. a) Binding site area of SHV-1 and co-crystal ligand (X: 11.729, Y: 37.5, and Z: -1.2519). b) The native ligand of SHV-1 before and after docking (Purple: before docking, blue: after docking) and RMSD 3.7^{o}A

Visualization of the Docking Results

The docking experiment evaluated the free energy of binding between inhibitors and the SHV-1 receptor, both through blind and specific docking approaches. Both methods yielded consistent results, identifying the top ten compounds with significant binding affinities, as illustrated in Figure 3a. The interactions between these active compounds and the receptor, specifically at the binding site, are primarily stabilized by hydrogen bonds and hydrophobic interactions, as shown in Figure 3b. The amino acids involved in these interactions exhibit significant similarities, as detailed in Tables 2 and 3. Paucidisine forms five hydrogen bonds with SHV-1 at the amino acid residues Ser-A: 130, Ser-A: 70, Asn-A: 132, Arg-A: 244, and Asn-A: 170. The (-)-19-Oxoisoeburnamine

establishes three hydrogen bonds with SHV-1 at Ser-A: 70, Ala-A: 237, and Asn-A: 132. Paucidactine A is hydrogen-bonded with SHV-1 at Ser-A: 130, Ser-A: 70, Ala-A: 237, and Asn-A: 132.

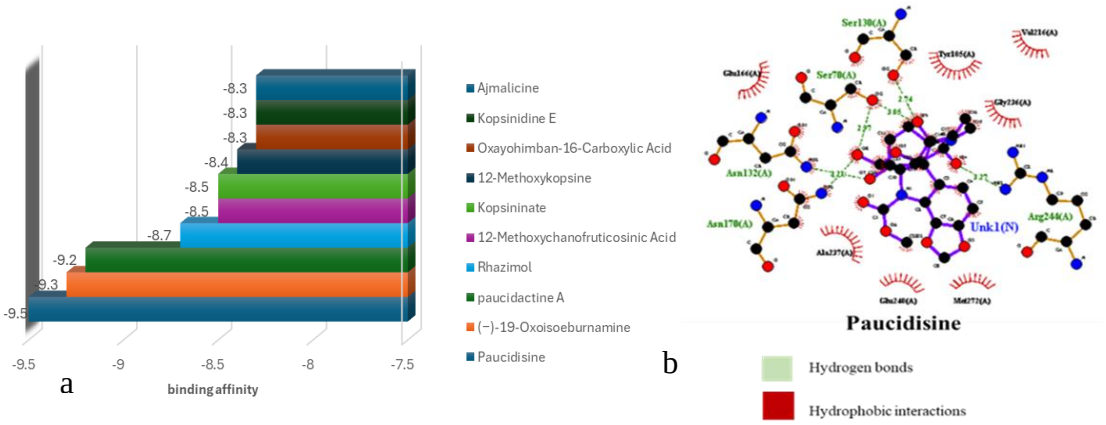

Figure 3. (a) The binding energy value (−kcal/mol) for the top ten MIA compound candidates resulted from docking analysis. (b) The interaction between paucidisine and SHV-1 protein. Hydrogen bonds and hydrophobic interaction support the interaction

Specific Ligand Interactions

Hydrophobic interactions are instrumental in further stabilizing these complexes by clustering the inner globular structures of proteins, thereby avoiding liquid environments (Gembloux dan Biophysique, 1995). Three lead compound candidates, as shown in Figure 4a-e, exhibited the best poses: Paucidisine, (-)-19-Oxoisoeburnamine, and paucidactine A. They yielded the lowest values and were found to be the most effective inhibitors of SHV-1.

The strength of hydrogen bonds formed with amino acid residues is a key factor in the formation of strong interactions. The more hydrogen bonds formed, the stronger the interactions, leading to lower energy scores and greater stability (Suhartono et al., 2019). (Głowacki et al., 2013), Hydrogen bonds involve interactions between hydrogen atoms and atoms such as fluorine (F), nitrogen (N), and oxygen (O) to which they are covalently bonded. This finding aligns with more recent studies (Głowacki et al., 2013). Three main criteria are essential for molecular docking: bond intensity, molecular linkages, and bond characterization. Lead compounds typically exhibit low bond energies, strong hydrogen bonds, and favorable drug-likeness profiles (Prasanth et al., 2021). In this study, each top ligand displayed varying numbers of hydrogen bonds at different amino acid residues (Table 2).

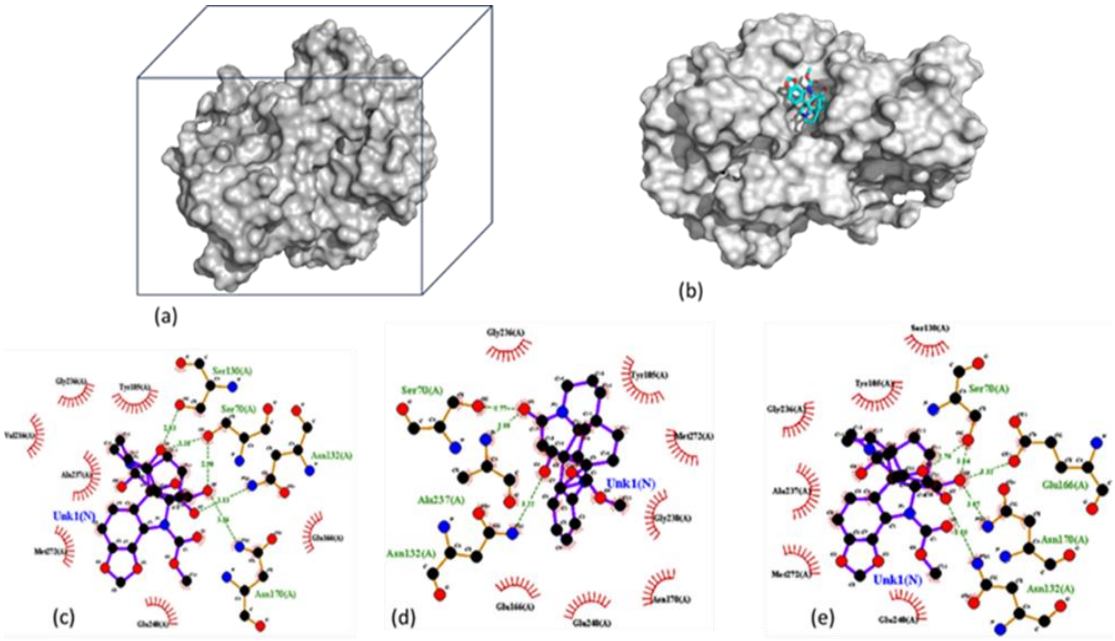

Figure 4. Docking position on SHV-1 protein. (a) Blind docking, (b) specific docking, (c) Paucidisine, (d) (-)-19-Oxoisoeburnamine, (e) paucidactine A on shv-1 protein.

Table 2. Hydrogen bond between SHV-1 and native ligand

Compound name	Hydrogen bonds									
	Residues									
	Lys234	Ser130	Ser70	Ala237	Asn132	Arg244	Thr235	Asn170	Glu166	Lys73
Native ligand (1OG)	O	O	O	O	O	O	O	X	X	X
Paucidisine	X	O	O	X	O	O	X	O	X	X
(−)-19-Oxoisoeburnamine	X	X	O	O	O	X	X	X	X	X
Paucidactine A	X	O	O	O	O	X	X	X	X	X
Rhazimol	X	X	O	O	X	X	X	X	O	O
12-Methoxychano-fruticosinic Acid	X	O	O	O	O	X	X	X	X	X
Oxayohimban-16-carboxylic Acid	X	X	O	X	X	O	X	X	X	X
Kopsininate	X	X	X	X	O	X	X	O	X	X
Kopsininic Acid	X	X	X	X	O	X	X	O	X	X
Kopsinidine E	X	O	X	X	X	O	X	X	X	X
Alsmaphorazine B	X	O	O	O	O	X	X	X	X	X

*nd: not determined
O means exists, X means does not exist

Table 3 Hydrophobic interaction between SHV-1 and native ligand (continued)

Compound name	Hydrophobic interaction															
	Residues															
	Met 69	Gly 238	Tyr 105	Val 216	Gly 236	Ala 237	Asn 170	Met 272	Glu 240	Glu 166	Ser 130	Asn 132	Thr 167	Asp 104	Ser 70	Thr 235
Native ligand (1OG)	O	O	O	O	O	X	X	X	X	X	X	X	X	X	X	X
Paucidisine	X	X	O	O	O	O	X	O	O	O	X	X	X	X	X	X
(−)-19-Oxoisoeburnamine	X	O	O	X	O	X	O	O	O	O	X	X	X	X	X	X
paucidactine A	X	X	O	X	O	X	O	X	X	X	O	X	X	X	X	O
Rhazimol	X	X	O	O	X	X	O	X	O	O	O	O	O	O	X	X
12-Methoxychanofruticosinic Acid	X	X	O	O	X	X	O	X	O	X	X	X	X	X	X	X
Oxayohimban-16-Carboxylic Acid	X	X	O	X	O	X	O	X	X	X	X	O	O	O	X	O
Kopsininate	X	O	O	X	X	O	X	X	X	O	O	X	X	X	O	X
Kopsininic Acid	X	O	O	X	X	O	X	X	X	O	O	X	X	X	O	X
Kopsinidine E	X	X	O	O	O	O	O	O	O	X	X	X	X	X	X	O
Alsmaphorazine B	X	O	O	O	O	X	O	X	O	X	X	X	X	X	X	O

*nd: not determined

O means exist, X means does not exist

The identification of lead compounds holds promising implications for combating antibiotic resistance associated with SHV-1, offering a ray of hope in the battle against superbugs. The molecular docking analysis in this study identified Paucidisine, (-)-19-Oxoisoeburnamine, and Paucidactine A as the top three ligands against SHV-1 β-lactamase. This is the first report on the potential of MIA compounds to bind to the SHV-1 protein through *an in silico* study. A previous study reported the activity of a synthetic compound, avibactam, in inhibiting the SHV-1 protein (Krishnan et al., 2015). Therefore, the development of natural compounds such as Paucidisine, (-)-19-Oxoisoeburnamine, and Paucidactine, which show high affinity to SHV1, serves as a potential application in treating *K. pneumoniae*, offering a promising future in the fight against antibiotic resistance.

The observed binding energy trends in this study align with the activity of synthetic β-lactamase inhibitors such as tazobactam and avibactam. Indeed, these synthetic compounds, which also rely on strong hydrogen bonding with Ser70 and Asn132, combined with hydrophobic interactions near the Ω-loop region (de Sousa Coelho & Mainardi, 2021). The top three ligands identified in this study represent potential scaffolds for the development of novel β-lactamase inhibitors, addressing a critical need in public health. However, it is essential to acknowledge the limitations of our study, including the reliance on computational modelling. The need for experimental validation of three potential compounds through *in vitro* and *in vivo* studies is crucial to confirm

their inhibitory activity, pharmacokinetics, and safety, highlighting the importance of future research in this area.

CONCLUSION

The study underscores the remarkable potential of natural compounds in drug discovery. Leveraging advanced Bioinformatics resources and PyRx, we identified several potent molecules against the SHV-1 protein. The monoterpene indole alkaloids Paucidisine, (-)-19-Oxoisoeburnamine, and paucidactine A exhibited the best binding free energies while bonded to β-lactamase, opening the door for further optimization. This research not only demonstrates the power of nature in drug discovery but also paves the way for innovative product design and production initiatives that have the potential to revolutionize healthcare.

ACKNOWLEDGMENT

We extend our sincere gratitude to the INBIO Center and the Bioinformatics Research Center for their invaluable support and resources, which were instrumental in the successful completion of this research. We also express our special thanks to Dr. Setyanto Tri Wahyudi, whose insightful discussions and guidance were invaluable throughout the study. His expertise and input significantly enriched our research.

REFERENCES

Abbas, R., Chakkour, M., Zein El Dine, H., Obaseki, E. F., Obeid, S. T., Jezzini, A., … Ezzeddine, Z. (2024). General Overview of Klebsiella pneumonia: Epidemiology and the Role of Siderophores in Its Pathogenicity. *Biology*, *13*(2), 78. 10.3390/BIOLOGY13020078

Agu, P. C., Afiukwa, C. A., Orji, O. U., Ezeh, E. M., Ofoke, I. H., Ogbu, C. O., … Aja, P. M. (2023). Molecular docking as a tool for the discovery of molecular targets of nutraceuticals in diseases management. *Scientific Reports*, *13*(1), 1-18. 10.1038/S41598-023-40160

Alfaridza, A. N., Astuti, R. I., & Mubarik, N. R. (2025). Interaksi Molekuler Senyawa Kuersetin dan Eugenol terhadap Protein Regulator Lintasan Penuaan SIR2, pada

Khamir *Saccharomyces cerevisiae*. *Biota : Jurnal Ilmiah Ilmu-Ilmu Hayati*, *10*(1), 44-52. 10.24002/BIOTA.V10I1.6819

Assefa, M. (2022). Multi-drug resistant gram-negative bacterial pneumonia: etiology, risk factors, and drug resistance patterns. *Pneumonia*, *14*(1), 1-12. 10.1186/S41479-022-00096-Z

de Sousa Coelho, F., & Mainardi, J. L. (2021). The multiple benefits of second-generation β-lactamase inhibitors in treatment of multidrug-resistant bacteria. *Infectious Diseases Now*, *51*(6), 510-517. 10.1016/j.idnow.2020.11.007

Diekema, D. J., Hsueh, P. R., Mendes, R. E., Pfaller, M. A., Rolston, K. V., Sader, H. S., & Jones, R. N. (2019). The microbiology of bloodstream infection: 20-year trends from the SENTRY antimicrobial surveillance program. *Antimicrobial Agents and Chemotherapy*, *63*(7). 10.1128/AAC.00355-19

Ferdosi-Shahandashti, A., Pournajaf, A., Ferdosi-Shahandashti, E., Zaboli, F., & Javadi, K. (2024). Identification of beta-lactamase genes and molecular genotyping of multidrug-resistant clinical isolates of *Klebsiella pneumoniae*. *BMC Microbiology*, *24*(1), 1-8. 10.1186/S12866-024-03679-6/FIGURES/2

Gembloux, D., & Biophysique, C. De. (1995). The hydrophobic. *Review Literature And Arts of The Americas*, 535-540.

Głowacki, E. D., Irimia-Vladu, M., Bauer, S., & Sariciftci, N. S. (2013). Hydrogen-bonds in molecular solids-from biological systems to organic electronics. *Journal of Materials Chemistry*, *1*(31), 3742-3753. 10.1039/c3tb20193g

Ikuta, K. S., Swetschinski, L. R., Aguilar, G. R., Sharara, F., Mestrovic, T., Gray, A. P., … Naghavi, M. (2022). Global mortality associated with 33 bacterial pathogens in 2019: a systematic analysis for the Global Burden of Disease Study 2019. *The Lancet*, *400*(10369), 2221-2248. 10.1016/S0140-6736(22)02185-7

Jenkins, D. R. (2021). Nosocomial infections and infection control. *Medicine*, *49*(10), 638-642. 10.1016/J.MPMED.2021.07.007

Khan, H. A., Baig, F. K., & Mehboob, R. (2017). Nosocomial infections: Epidemiology, prevention, control and surveillance. *Asian Pacific Journal of Tropical Biomedicine*, *7*(5), 478-482. 10.1016/J.APJTB.2017.01.019

Krishnan, N. P., Nguyen, N. Q., Papp-Wallace, K. M., Bonomo, R. A., & Van Den Akker, F. (2015). Inhibition of *Klebsiella* β-Lactamases (SHV-1 and KPC-2) by Avibactam: A Structural Study. *PLOS ONE*, *10*(9), e0136813. 10.1371/JOURNAL.PONE.0136813

Liakopoulos, A., Mevius, D., & Ceccarelli, D. (2016). A review of SHV extended-spectrum β-lactamases: Neglected yet ubiquitous. *Frontiers in Microbiology*, *7*(SEP). 10.3389/fmicb.2016.01374

Liu, Y. P., Liu, Q. L., Zhang, X. L., Niu, H. Y., Guan, C. Y., Sun, F. K., … Fu, Y. H. (2019). Bioactive monoterpene indole alkaloids from *Nauclea officinalis*.

Bioorganic Chemistry, *83*, 1-5. 10.1016/j.bioorg.2018.10.013

Meng, X.-Y., Zhang, H.-X., Mezei, M., & Cui, M. (2011). Molecular Docking: A powerful approach for structure-based drug discovery. *Current computer-aided drug design*, *7*(2), 146. 10.2174/157340911795677602

Mohammed, A. E., Abdul-Hameed, Z. H., Alotaibi, M. O., Bawakid, N. O., Sobahi, T. R., Abdel-Lateff, A., & Alarif, W. M. (2021). Chemical diversity and bioactivities of monoterpene indole alkaloids (Mias) from six Apocynaceae genera. *Molecules*, *26*(2), 1-67. 10.3390/molecules26020488

Parawidnyaningsih, P. A. A., Masfufatun, Listyawati, A. F., Kuntaman, K., & Sudibya, A. (2023). Detection of Enterobacteriaceae lactose fermenter bacteria producing extended spectrum beta-lactamase (ESBL) in food samples at Surabaya. *BIOMA: Jurnal Ilmiah Biologi*, *12*(2), 38-45. 10.26877/bioma.v11i2.16618

Prasad, N., Ramteke, P., Dholia, N., & Yadav, U. C. S. (2018). *Therapeutic interventions to block oxidative stress-associated pathologies*. *Immunity and Inflammation in Health and Disease: Emerging Roles of Nutraceuticals and Functional Foods in Immune Support*. Elsevier Inc. 10.1016/B978-0-12-805417-8.00027-5

Ramírez, D., & Caballero, J. (2018). Is It Reliable to Take the Molecular Docking Top Scoring Position as the Best Solution without Considering Available Structural Data? *Molecules*, *23*(5), 1038. 10.3390/MOLECULES23051038

Sahu, D., Rathor, L. S., Dwivedi, S. D., Shah, K., Chauhan, N. S., Singh, M. R., & Singh, D. (2024). A Review on Molecular Docking As an Interpretative Tool for Molecular Targets in Disease Management. *Assay and Drug Development Technologies*, *22*(1), 40-50. 10.1089/ADT.2023.060,

Sepehri, N. Z., Parvizi, M. M., Habibzadeh, S., & Handjani, F. (2022). Lettuce as an Effective Remedy in Uremic Pruritus: Review of the Literature Supplemented by an In Silico Study. *Evidence-based Complementary and Alternative Medicine*. Hindawi Limited. 10.1155/2022/4231854

Suhartono, E., Noor, Z., Edyson, Budianto, W. Y., & Idroes, R. (2019). Effect of chronic lead exposure on bone using ATR-FTIR spectroscopy. *AIP Conference Proceedings*, *2108*(June). 10.1063/1.5110000

Syarifah, I. F., Suryani, Y., Adzani, G. G., Kurniawan, I. D., & Taupiqurrohman, O. (2022). Pharmacophore Analysis of Monoterpene *Melaleuca leucadendra* as an Inhibitor for 3CLPro of the SARS-CoV-2. *Jurnal Biodjati*, *7*(2), 259-267. 10.15575/BIODJATI.V7I2.20496

Tallei, T. E., Tumilaar, S. G., Niode, N. J., Fatimawali, Kepel, B. J., Idroes, R., … Emran, T. Bin. (2020). Potential of Plant Bioactive Compounds as SARS-CoV-2 Main Protease (Mpro) and Spike (S) Glycoprotein Inhibitors: A Molecular Docking Study. *Scientifica*, *2020*. 10.1155/2020/6307457

Tooke, C. L., Hinchliffe, P., Bragginton, E. C., Colenso, C. K., Hirvonen, V. H. A., Takebayashi, Y., & Spencer, J. (2019). β-Lactamases and β-Lactamase Inhibitors

in the 21st Century. *Journal of Molecular Biology*, *431*(18), 3472. 10.1016/J.JMB.2019.04.002

Vasconcelos, P. G. S., Lee, K. M., Abuna, G. F., Costa, E. M. M. B., & Murata, R. M. (2024). Monoterpene antifungal activities: evaluating geraniol, citronellal, and linalool on *Candida* biofilm, host inflammatory responses, and structure–activity relationships. *Frontiers in Pharmacology*, *15*, 1394053. 10.3389/FPHAR.2024.1394053

Yuan, S., Chan, H. C. S., & Hu, Z. (2017). Using PyMOL as a platform for computational drug design. *Wiley Interdisciplinary Reviews: Computational Molecular Science*, *7*(2), e1298. 10.1002/WCMS.1298

Zhu, J., Wang, T., Chen, L., & Du, H. (2021). Virulence Factors in Hypervirulent *Klebsiella pneumoniae*. *Frontiers in Microbiology*, *12*. 10.3389/FMICB.2021.642484